RSC Advances

PAPER

View Article Online
View Journal | View Issue

Cite this: *RSC Adv.*, 2017, **7**, 2193

Experimental and kinetic studies of coal–CO_2 gasification in isothermal and pressurized conditions

Lang Liu,*[ab] Yan Cao,*[b] Qingcai Liu[c] and Jian Yang[c]

This study is to explicate the reaction mechanisms and kinetics of high-pressure char CO_2 gasification *via* a joint experimental and model simulation approach. The high-pressure char–CO_2 gasification reactions were studied experimentally using a high pressure thermo-gravimetric analyzer (HP-TGA). The results showed that the char CO_2 gasification rate experienced an initially slow increase until the carbon conversion reached 0.6 (Zone I), when a rapid increase in the carbon conversion increased to 0.9 (Zone II). Further gasification reaction, corresponding to a carbon conversion efficiency above 0.9 (Zone III), finally, presented a sharp decrease in kinetics. For more accurate interpretation of the experimental char–CO_2-gasification kinetics and mechanisms, we found a proven kinetic model could be derived based on the random pore model and mixed model, which specifically predicate the studied gasification reaction and its critical kinetics parameters of the Zone I and II, respectively. The developed kinetics model, assembling major parameters (including char structures, pressure order, reaction order, activation energy and pre-exponential factor) was found to be in good agreement with the experimental results, covering wide realistic gasification operation conditions. This study revealed an optimal carbon conversion range with rational gasification kinetics, which can be estimated based on an accurate kinetics model.

Received 29th October 2016
Accepted 8th December 2016

DOI: 10.1039/c6ra25994d

www.rsc.org/advances

1. Introduction

Chemical looping combustion and gasification (CLC&G) have been suggested to be one of the most promising technologies of the inherent separation of CO_2 with a reduced energy penalty. Oxygen carriers, replacing air, are used as an oxygen source, thus preventing mixing of nitrogen into the CO_2 stream. Recently, several investigations have focused on the use of solid fuel (such as coal) as the potential fuels in the CLC&G system.[1–6] There are two potential reaction paths between the oxygen carrier and coal: a direct reaction between oxygen carriers and solid fuels, and an indirect reaction between the oxygen carriers and gaseous intermediates (syngas) from the gasification of solid fuels. Indirect reduction has been identified as the major reaction path between oxygen carriers and solid fuels because of the low contact efficiency between coal and oxygen carriers, solid–solid reactions occur in the direct reaction path. Therefore, the char gasification is the rate-determining process in the coal-direct chemical looping combustion and gasification. Therefore, it is important to investigate and further improve to the kinetics of the char gasification in the CLC&G system.

The general approach to improve the kinetics of the char gasification is the high temperature and pressurized operations.[7] Many factors have been proved to affect kinetics of coal char gasification, including char ranks, particle sizes, temperatures, the partial pressures of the reactant gases and the total system pressure, as well as gasification agents (likely O_2, H_2O and/or CO_2).[8–12] The water is the mostly used gasification agent, which is more reactive than CO_2. However, water is also resource-limited and energy-intensive than CO_2. The exploration to use CO_2 as gasification agent may contribute to reduce the dependence of water usage in the coal gasification process, and thus is significant in the industry gasification application. Recently, experimentally the CO_2 gasification mechanisms have been investigated,[13–20] and their regular empirical reaction models have been addressed, such as the volume model,[21] the hybrid model[22] and the random pore model.[19,23–26] Among of these kinetic models, the random pore model seemed the most practical one, addressing the growth and coalescence of the char structure during the char gasification process. However, it is feasible to describe the maximum reaction rate at low conversion levels, but difficult to explain the intrinsic reaction rate throughout the char gasification. For example, Roberts *et al.*[13,16,27,28] studied factors such as temperature, pressure, the

[a]*Guizhou Institute of Technology, Chemical Engineering Institute, Guiyang, Guizhou, 550003, China. E-mail: l.liu.git@qq.com*

[b]*Institute for Combustion Science and Environmental Technology, Chemistry Department, Western Kentucky University, Bowling Green, KY 42101, USA. E-mail: yan.cao@wku.edu*

[c]*College of Material Science & Engineering, Chongqing University, Shapingba, Chongqing 400044, China*

gasification agent and CO inhibition, on the intrinsic reaction rate of the char gasification. They assumed the intrinsic reaction rate can be found and studied when the char carbon conversion was around 0.1. The intrinsic reaction rate of the gasification is one when a chemical-reaction controlling condition is applied. Models that are used to predict high temperature char gasification behavior usually have a chemical reaction component that accounts for the variation in intrinsic reaction rate with operating temperature and pressure. This component is usually combined with the analysis of the effects of the surface chemical reaction rate and pore diffusion limitations to arrive at an overall gasification rate over a wide range of temperatures.

In our previous paper,[29] the high-pressure char–CO_2 gasification reactions were studied experimentally using a high pressure thermo-gravimetric analyzer (HP-TGA). The results showed that the gasification rate initially experienced a slow increase, and followed by a rapid increase, and finally a decrease corresponding to increasing the carbon conversion efficiency. Also, the structural and crystalline features of gasified chars at different conversions efficiencies are well characterized using BET, XRD, Raman spectroscopy, FTIR and SEM. It was found that the char structure changes of interest were generally accepted as having major impacts on kinetics of char gasification, especially for the slow CO_2 gasification process. Authors, in this manuscript, attempted to demonstrate this type of interaction between char kinetics and physical and chemical properties of char. But, the complete kinetics models regarding the kinetics of the selected coal have not been presented in our previous paper.

This paper was focused on the chemical reaction component of such models, and how it can be practically applied while still accurately describing the intrinsic reactivity behavior of chars throughout the gasification process over a wide range of operating temperature and pressure.

The primary objective of this paper was to develop a practical combined model to present the intrinsic reaction kinetics of the char gasification using CO_2 as the gasification agent under the elevated temperatures and pressures by. Experiments have been carried out in a pressurized thermo-gravimetric analyzer. The temperature range was controlled isothermally between 950 to 1150 °C, and pressure between up to 3.0 MPa.

2. Experimental and model method development

2.1 Materials

A Kentucky Bituminous coal was used in the experiments; the proximate analyses and ultimate analysis of the selected coal are listed in the Table 1, and the coal particles were sieved to around 200 μm in this study. The experiments were carried out consecutively in the pressurized thermo-gravimetric analyzer (TGA-HP150S), which has been described in our previous studies.[29,30] In the experiment, 500 mg coal char was added in a crucial boat, firstly pressured to the designed pressure, heated in N_2 at 1000 mL min^{-1} to a reaction temperature with the rate of 20 °C min^{-1}, and then isothermal for half an hour under the nitrogen atmosphere. After the char preparation process, the gas was switched to CO_2 with the concentration of 25% and 100% by mole at 1000 mL min^{-1}. The TGA collected the mass of the samples at different times automatically during the char gasification process.

According to the data from the thermo-gravimetric analyzer, the carbon conversion efficiency ($x(t)$) of char defined as the ratio of the gasified char at any time t to the initial char can be calculated as

$$x(t) = \frac{w_0 - w}{w_0 - w_{ash}} \times 100\% \quad (1)$$

The intrinsic reaction rates (ρ) were calculated as

$$\rho = \frac{dx}{(1-x)dt} \quad (2)$$

where, w_0—the initial mass of char; w—the instantaneous char mass at reaction time t; w_{ash}—the mass of ash.

2.2 Kinetic analysis

2.2.1 Langmuir–Hinshelwood rate equation. The gasification reaction with CO_2 can be presented by the Langmuir–Hinshelwood model:[19,31,32]

$$C + CO_2 \leftrightarrow C(O) + CO,\ k_1,\ k_2 \quad (3)$$

$$C(O) \rightarrow CO,\ k_3 \quad (4)$$

The intrinsic reaction rates (ρ) were described by the Langmuir–Hinshelwood rate equation:

$$\rho = \frac{[C_t]k_1 P_{CO_2}}{1 + \frac{k_2}{k_3}P_{CO} + \frac{k_1}{k_3}P_{CO_2}} \quad (5)$$

where, C(O)—the reaction intermediate surface complexes; k_1—the rate constant for the forward reaction of reaction (3); k_2—the rate constant for the reverse reaction of reaction (3); k_3—the rate constant for reaction (4); P_{CO}, P_{CO_2}—the partial pressure of CO and CO, respectively; $[C_t]$—the total concentration of active sites.

Table 1 Proximate and ultimate analysis of the Kentucky Bituminous coal (wt%)

	Proximate analysis				Ultimate analysis (dry basis)				
	Moisture	Fixed carbon	Volatiles	Ash	C	H	N	O	S
Coal	5.06	49.46	35.02	10.46	65.52	4.52	1.43	13.94	3.57

In the experiments, $P_{CO_2} \gg P_{CO}$ and the influence of CO on the reaction is little. So the partial pressure of CO can be ignored in our experiment, and the eqn (5) was simplified to become

$$\frac{1}{\rho} = \frac{1}{[C_t]k_1 P_{CO_2}} + \frac{1}{[C_t]k_3} \quad (6)$$

So, the value for k_1/k_3 (the intercept divided by the gradient) can be got by charting $1/\rho$ *versus* $1/P_{CO_2}$.

2.2.2 Random pore model. The random pore model[24,33] was chosen since the char was characterized by the presence of fine pores and cracks,[19] which can contribute to intra-particle gas penetration and subsequent particle structural changes.[19,24]

The overall reaction rate is[24]

$$\frac{dx}{dt} = A_0(1-x)P_A{}^n \exp\left(-\frac{E_I}{RT}\right)\sqrt{1-\psi\ln(1-x)} \quad (7)$$

where, n is the pressure order with respect to the reactant gas and can be calculated by[13,34,35]

$$n = e^{-\frac{\frac{k_1}{k_3}P_{CO_2}}{1+\frac{k_1}{k_3}P_{CO_2}}} \quad (8)$$

ψ is the structural parameter characteristic of the initial char structure and defined as

$$\psi = \frac{4\pi L_0(1-\varepsilon_0)}{S_0{}^2} \quad (9)$$

here, S_0—initial surface area; L_0—the total pore length per unit volume; ε_0—the initial porosity.

The structural parameter (ψ) has been determined *via* BET results and image analysis,[24,36] and *via* experimental reaction rate results. However, as for the non-uniform pore size distribution char, BET measurements and image analysis were not accurate enough because of the approximations required to describe the non-uniformity of the pore sizes as well as the accuracy of the pore size estimates within the micro-pore range.[19] Lu *et al.*[37] estimated this parameter from the maximum of experimental reaction rate curves obtained from conversion results. These estimates, however, depend on the accuracy of the numerical estimation of the maxima are limited to a very narrow carbon conversion range. This problem was overcome by regression with the unknown structural parameter based on experimental results by other authors.[19]

In this paper, this parameter was estimated by the method as follow.

Rearrangement of the equation provides the following

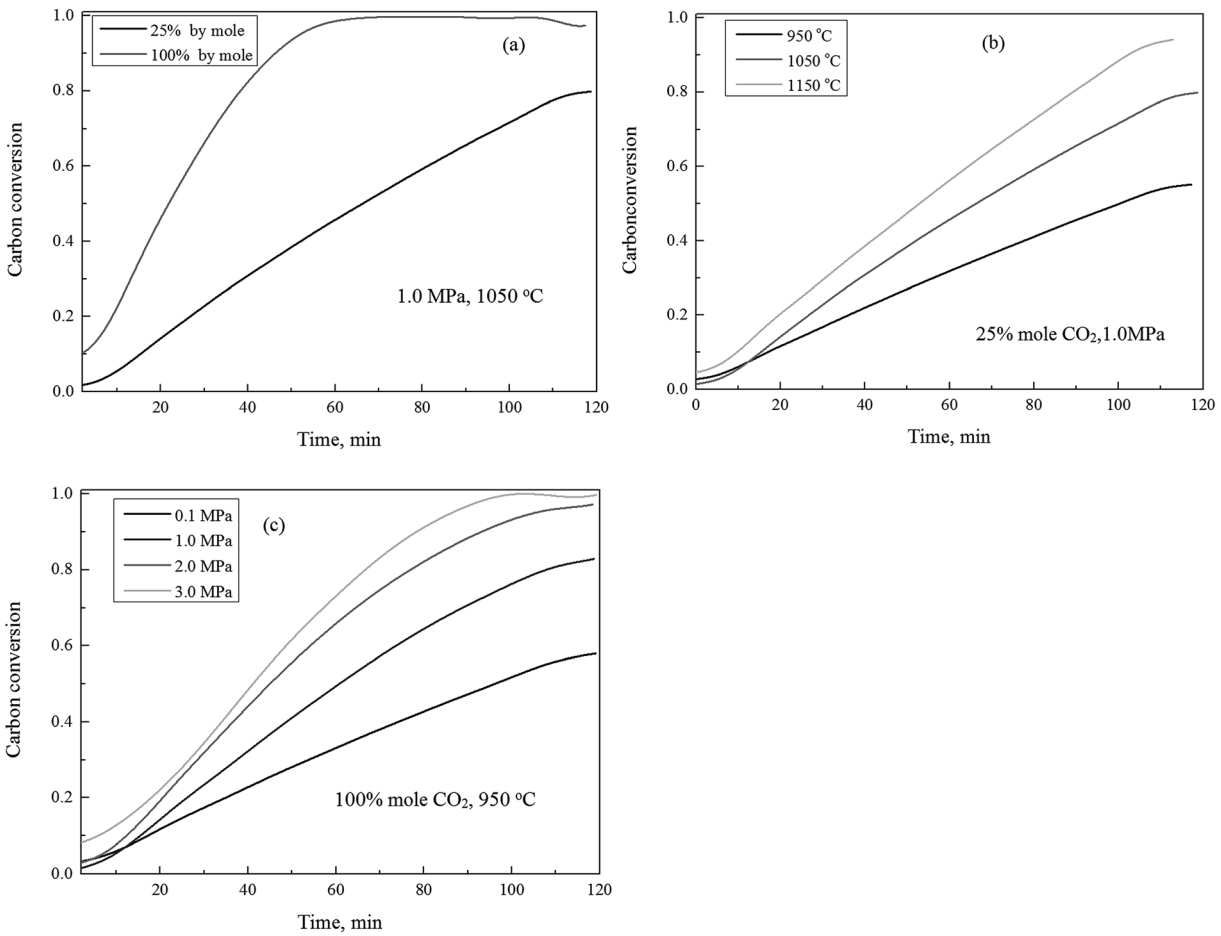

Fig. 1 The effect of CO_2 concentration, T and P on the gasification rate.

$$\rho = A_0 P_A{}^n \exp\left(-\frac{E_I}{RT}\right)\sqrt{1-\psi\ln(1-x)} \quad (10)$$

If we defined $k_s = A_0 P_A{}^n \exp\left(-\frac{E}{RT}\right)$, $x' = \ln(1-x)$, while

$$k_I = A_0 \exp\left(-\frac{E}{RT}\right) \quad (11)$$

We can get

$$\rho^2 = k_s{}^2 - k_s{}^2\psi x' \quad (12)$$

With regression analysis, ψ can be calculated by using the linear regression model between ρ^2 and $k_s{}^2$. This is likely one of the reasons for ensuring that conversion levels are constant when undertaking investigations of char gasification intrinsic reaction kinetics, in particular when the determination of specific and intrinsic rate constants is required.[16] Roberts *et al.*[13,16,27] investigated the intrinsic reaction rates reasonably using the specific reaction rates when the carbon conversion efficiency was 0.1. In this study, the carbon conversion efficiency below 0.1 was the initial intrinsic-rate-controlling stage, and thus was applied to analyze the initial intrinsic kinetics of the selected char.

2.2.3 Mixed model. The mixed model was used to model the kinetic of the char gasification and the rate of CO_2 gasification can be expressed as

$$\rho = k_{II} P_A{}^n (1-x)^{m-1} \quad (13)$$

While,

$$k_{II} = A_i \exp\left(-\frac{E_{II}}{RT}\right) \quad (14)$$

where A_i is the pre-exponential factor, E_{II} is the activation energy and m is the reaction order.

If we defined

$$k_r = A_i P_A{}^n \exp\left(-\frac{E_{II}}{RT}\right) \quad (15)$$

We can get

$$\ln\rho = \ln k_r + (m-1)\ln(1-x) \quad (16)$$

3. Results and discussion

3.1 Experimental results

The gasification reactivity of the char using CO_2 as gasification agent, in response to variation of the concentrations of carbon dioxide, temperatures and pressures, were shown in Fig. 1. Fig. 1(a) shows the carbon conversion efficiency *versus* time as the CO_2 concentration varied between 25% and 100% (by mole ratio) at 1.0 MPa and 1050 °C. It can be observed that the carbon conversion efficiency was sensitive in response to the variation of CO_2 concentrations. The increase of concentration of CO_2 leads the increase of the carbon conversion throughout the char gasification process.

The effect of temperature on the char gasification was pretty straightforward, as shown in Fig. 1(b). The elevation of gasification temperatures generally resulted in the increase of the carbon conversion efficiency under constant pressures and CO_2 concentrations throughout the char gasification process. As

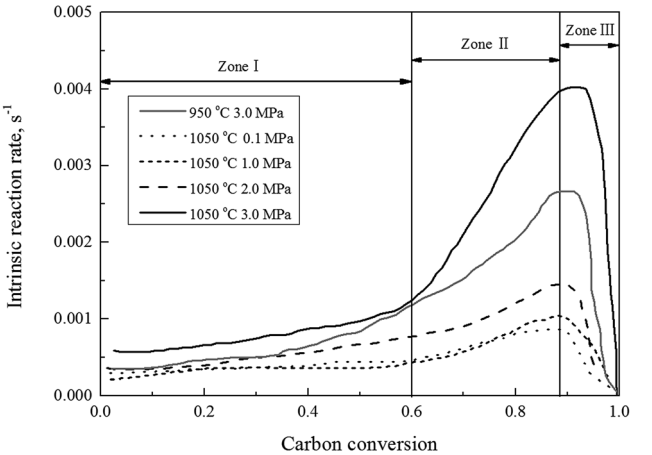

Fig. 2 The gasification rate *versus* the carbon conversion efficiency using 100% CO_2 at selected operating conditions.

Table 2 The values of k_1/k_3 of the char sample under different conditions

Temperature	Carbon conversion	k_1/k_3	Correlation coefficient
950 °C	10%	1.263	0.99
	20%	0.968	0.95
	30%	0.927	0.94
	40%	0.868	0.951
	50%	0.811	0.95
	60%	0.750	0.96
	70%	0.762	0.96
	80%	0.766	0.97
	90%	0.781	0.96
1050 °C	10%	0.78	0.99
	20%	0.81	0.99
	30%	0.82	0.98
	40%	0.71	0.98
	50%	0.69	0.98
	60%	0.74	0.98
	70%	0.77	0.97
	80%	0.65	0.95
	90%	0.76	0.98
1150 °C	10%	0.616	0.98
	20%	0.539	0.97
	30%	0.522	0.98
	40%	0.452	0.96
	50%	0.538	0.98
	60%	0.527	0.98
	70%	0.455	1
	80%	0.474	0.94
	90%	0.525	0.97

shown in Fig. 1(c), the effect of pressure on char gasification was similar to that of temperature, the increase of the gasification pressures resulted in the increase of the carbon conversion efficiency throughout the complete char conversion, which was consistent to published studies.[19,38]

Fig. 2 shows the gasification rate *versus* the carbon conversion efficiency using 100% CO_2 as gasification agent at selected operating conditions. It was observed that the gasification rate initially experienced a slow increase (Zone I), and followed by a rapid increase (Zone II), and finally a decrease (Zone III) corresponding to increasing the carbon conversion efficiency. The char CO_2 gasification rates differed at these three stages should be associated with major rate controlling factors individually or jointly, such as rates of pore diffusions for reactants and gas products, the surface chemical adsorption, and intrinsic reaction. It was well known that the char structural parameters, such as specific surface area and atomic structure, subject to significant changes during the carbon conversion of the gasified char under a wide gasification conditions.[16,39–41] Our previous studies[29] presented, that changes of both the surface area and pore volume of the gasified char played major roles on the gasification reaction rate during the char–CO_2 gasification. In the initial stage of the char gasification, the surface of char was revealed coarse with many small embossed parts, identified partially as small surface bulge and partially the initial underdeveloped pores structures. The initial pore opening on the char surface, surly resulted in that more pores underneath char surface were accessible by the gasification agent to let the process of pore openings move on. The outcomes lead more char participation in gasification process and the gasification rates speed-up until the carbon conversion efficiency reaching to around 0.9. The pore structures of the gasified char and its development solely dominated the gasification rate, while the intrinsic surface reaction was also involved. As presented later this study, the kinetic of Zone I and II can be well modeled by random pore model and mixed model, respectively. In the final stage of gasification as the carbon conversion efficiency above 0.9, the pore of the char particles started to collapse and disappeared and the reaction rate was controlled by the surface chemical reaction. Another evidence[29] from Raman spectroscopy study supported the domination effect of the surface chemical reaction, that was the graphitization of carbon residue in the gasified char. Therefore, the char gasification when the carbon conversion efficiency above 0.9 was not suggested.

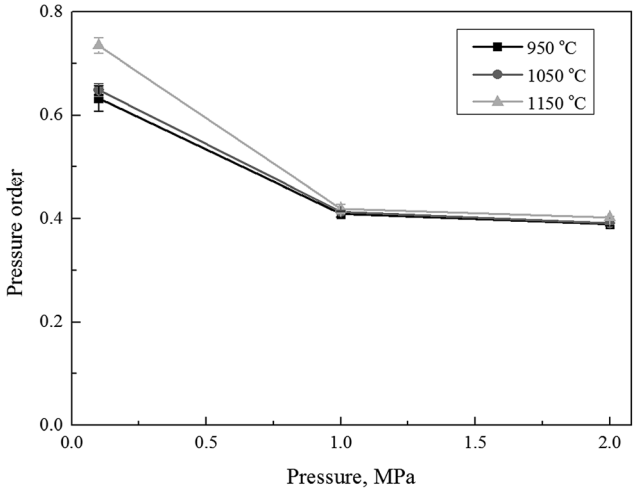

Fig. 3 The calculated pressure order at different pressure.

3.2 Kinetic model of char gasification

3.2.1 The determination of the pressure order. The values of k_1/k_3 (in eqn (6)), correlating the gasification rate *versus* CO_2 partial pressure made in the absence of CO, *versus* the carbon conversions at a temperature range between 950 and 1050 °C can be calculated from experimental results. Table 2 was a summary of the calculated k_1/k_3 values and the correlation coefficients. It can be seen that the value of the correlation coefficients were greater than 0.94, indicating that it is feasible to calculate the vales of the k_1/k_3 based on our derived model. The majority calculated k_1/k_3 values at different carbon conversion efficiencies were found to be generally below 1.0,

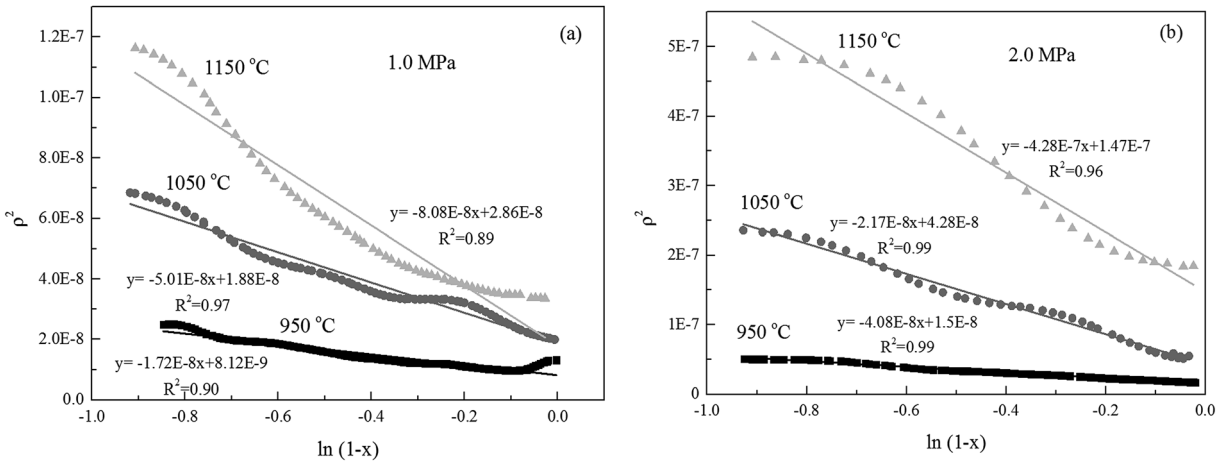

Fig. 4 The charts of ρ^2 *versus* $\ln(1-x)$ in Zone I.

clearly indicating that the char gasification rate was controlled by the rate of desorption of the surface intermediate complexes. This was coincided to the same phenomenon found in char gasification at atmospheric pressure of published studies.[34,42]

The obtained data, listed in Table 2, were consequently used in eqn (8) to calculate the extent of pressure order (n). The calculated pressure order (n), with respect to the partial pressure of the reactant gas at the different carbon conversion efficiency during the char gasification, was shown in Fig. 3. The calculated pressure order of the selected char in this study was found almost constant at about 0.4 under operational pressures of 1.0 and 2.0 MPa, but increased to 0.63–0.73 as the operational pressure dropped to 0.1 MPa. This was roughly in agreement to a pressure order in 0.5 ($\pm$0.04) obtained by Everson R. C. *et al.*[19] and 0.53 by Lu and Do.[37] The difference of pressure order parameters should be largely attributed to sources of char in different studies. The expanded literature studies revealed there was actually no consensus in previous studies regarding the pressure orders of very different coal samples and their corresponding chars at different operating conditions. The reported pressure order parameter of chat gasification was largely varied within a range between 0.2 and 0.8.[19] However, it's true that the pressure order did decrease under an increase of operational pressures.[43] Fig. 3 also implied that the temperature had little influence on the pressure order of the char gasification when the operational pressure was controlled constantly at 1.0 and 2.0 MPa.

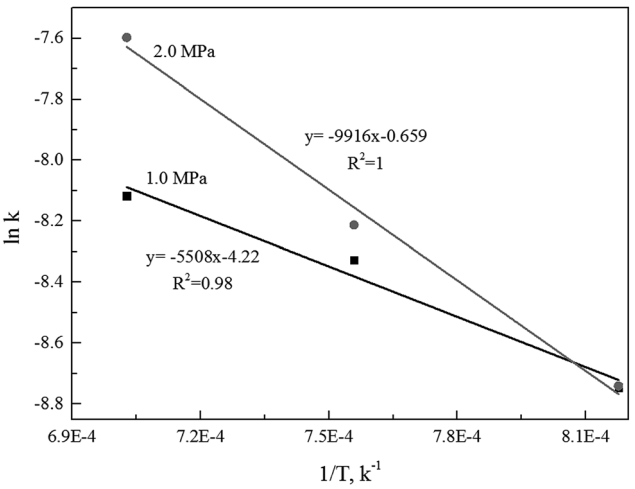

Fig. 5 The curves of the linear regression of gasification reaction rate.

3.2.2 Determination of kinetic parameters. The random pore model described in the Experimental section was used to estimate the structural parameter of the Zone I (x < 0.6). The gasification rate when carbon conversion efficiency below 0.6, called Zone I. It has been proved that the calculated pressure orders were not a constant at 0.1 MPa in the previous section, and thus the eqn (12) could not be applied for the char gasification at 0.1 MPa. The charts of ρ^2 *versus* $\ln(1-x)$ were shown in Fig. 4. The structural parameter ψ equal led to 2.5 ($\pm$0.4). Many previous studies developed alternative methods to calculate ψ. These included the Kajitani[18] method to determine the structural parameter using the measured BET results, and the Ochoa method[17] to calculate ψ using the gasification conversion efficiency (x) at the char maximum reaction rate, as well as the Everson method[19] to estimate this parameter using results of the overall reaction rate.

The linear regression model could be applied to determine the activation energy (E) and frequency factor (A_0). Fig. 5 shows the curves of the linear regression of gasification reaction rate. The analyzed values of kinetics parameters were summarized in Table 3. Table 3 clearly presented that both the activation energy and frequency factor increased when operation pressures increased.

Table 3 Gasification rate equations and kinetic parameters for the char gasification

Zone I : $\rho = A_0 P_A{}^n \exp\left(-\frac{E_I}{RT}\right)\sqrt{1-\psi\ln(1-x)}$, $(0 < x \leq 0.6)$

Pressure, MPa	Temperature, °C	Reaction rate constant, k	Structural parameter, ψ	Activation energy, E_I (kJ mol^{-1})	Frequency factor, A_I (s^{-1} MPa^{-n})	Pressure order, n
1.0 MPa	950	3.43×10^{-5}	2.11	45.8	0.015	0.42
	1050	5.21×10^{-5}	2.66			
	1150	6.43×10^{-5}	2.82			
2.0 MPa	950	3.57×10^{-5}	2.72	82.4	0.52	0.41
	1050	6.06×10^{-5}	2.91			
	1150	1.12×10^{-4}	2.91			

Zone II: $\rho = k_{II} P_A{}^n (1-x)^m$, $(0.6 < x \leq 0.9)$

Pressure, MPa	Temperature, °C	Reaction rate constant, k_{II}	Reaction order, m	Activation energy, E_{II} (kJ mol^{-1})	Frequency factor, A_{II} (s^{-1} MPa^{-n})	Pressure order, n
1.0 MPa	950	1.12×10^{-4}	0.53	35.93	0.011	0.42
	1050	2.09×10^{-4}	0.53			
	1150	2.44×10^{-4}	0.39			

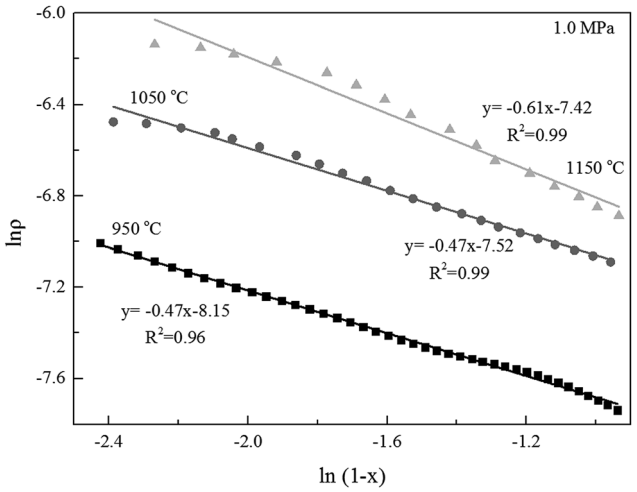

Fig. 6 The charts of ln ρ *versus* ln$(1 - x)$ in the Zone II.

Alternatively, the mixed model described in the Experimental section was used to estimate kinetics of the Zone II ($0.6 < x < 0.9$) of the char gasification at 1.0 MPa. The charts of ln ρ *versus* ln$(1 - x)$ were shown in Fig. 6, the results of the calculations, providing k_r and reaction order values of the char gasification at different operational conditions. Fig. 7 showed Arrhenius plots of gasification rates in the Zone II. Because continuous gasification rates were obtained with the TGA, the gasification rate when carbon conversion efficiency between 0.6 and 0.9, where the reaction rate could be controlled by pore diffusion. Table 3 summarized the estimated kinetic parameters of the Zone II.

An overall kinetic model of the char gasification under the isothermal and pressurized conditions could be determined, after aforementioned factors (including pressure order, structural parameter, reaction order, and activation energy and frequency factor) were derived from the experimental results based on gasification mechanism and proper kinetics model.

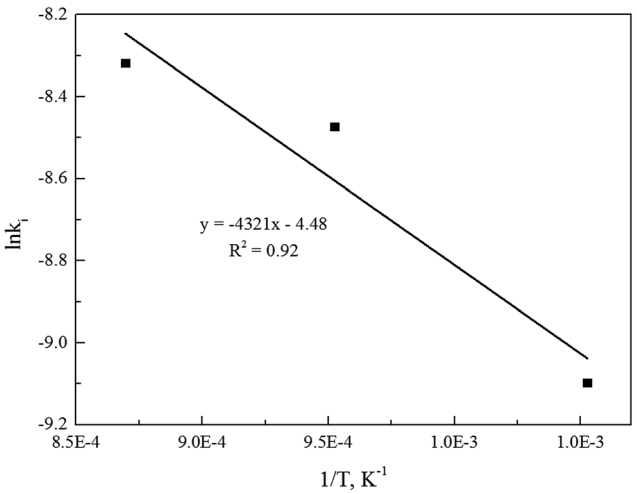

Fig. 7 Arrhenius plots of gasification rates in the Zone II.

The kinetic parameters of the intrinsic reaction kinetics of the char gasification at 1.0 MPa, has been summarized in Table 3.

4. Conclusions

The kinetics of the char–CO_2 gasification reactions at high pressures were studied experimentally using a pressurized thermo-gravimetric analyzer (HP-TGA). The results showed that the gasification rate experienced an initially slow increase when the carbon conversion below 0.6 (Zone I), then a rapid increase when the carbon conversion between 0.6 and 0.9 (Zone II) and finally a decrease when carbon conversion above 0.9 (Zone III) corresponding to the carbon conversion efficiency. The combination of the L–H model, the *n*th order model, the random pore model and mixed model were initially used to simulate the intrinsic reaction kinetics of the char–CO_2 gasification.

The results implied that it was incompatible to use a combined model to thoroughly present the complete conversion of the char–CO_2 gasification, but seemed useful to determine the intrinsic reaction kinetics of the char gasification by two different combined models at Zone I and II. For more accurate interpretation of kinetics of the char gasification, based on the random pore model and mixed model were developed by the predicated intrinsic reaction parameters, which was found in a good agreement with the TGA data under different operating conditions. Also, the structural parameter of char, reaction order, the pressure order, the activation energies and the intrinsic pre-exponential factor were determined.

Acknowledgements

This study was supported by the U.S. Department of Agriculture (5040-12630-005-00D), the 2014–2016 NSF RSP&RSP EPSCoR program (the National Science Foundation under Cooperative Agreement No. 1355438), and the support from the Science and Technology Foundation of Guizhou Province (No. qian ke he J zi [2015]2059) and the NSF-CHE-MRI under the Award ID of 1338072.

References

1 L. Zeng, F. He, F. Li and L.-S. Fan, Coal-direct chemical looping gasification for hydrogen production: reactor modeling and process simulation, *Energy Fuels*, 2012, **26**, 3680–3690.

2 Y. Cao, B. Casenas and W.-P. Pan, Investigation of chemical looping combustion by solid fuels. 2: Redox reaction kinetics and product characterization with coal, biomass, and solid waste as solid fuels and CuO as an oxygen carrier, *Energy Fuels*, 2006, **20**, 1845–1854.

3 Y. Cao and W.-P. Pan, Investigation of chemical looping combustion by solid fuels. 1: Process analysis, *Energy Fuels*, 2006, **20**, 1836–1844.

4 C. Linderholm and M. Schmitz, Chemical-looping combustion of solid fuels in a 100 kW dual circulating fluidized bed system using iron ore as oxygen carrier, *J. Environ. Chem. Eng.*, 2016, **4**, 1029–1039.

5 L. Liu, Q. Liu, Y. Cao and J. Yang, Investigation of sintered iron ore fines as an oxygen carrier in chemical looping combustion, *J. Therm. Anal. Calorim.*, 2016, 1–11.
6 C. Yan, W. Yang, J. T. Riley and W. P. Pan, A novel biomass air gasification process for producing tar-free higher heating value fuel gas, *Fuel Process. Technol.*, 2006, **87**, 343–353.
7 F. Li, Q. Yan, J. Huang, J. Zhao, Y. Fang and J. Wang, Lignite-char gasification mechanism in mixed atmospheres of steam and CO_2 at different pressures, *Fuel Process. Technol.*, 2015, **138**, 555–563.
8 D. Sutton, B. Kelleher and J. R. Ross, Review of literature on catalysts for biomass gasification, *Fuel Process. Technol.*, 2001, **73**, 155–173.
9 W. Zhu, W. Song and W. Lin, Catalytic gasification of char from co-pyrolysis of coal and biomass, *Fuel Process. Technol.*, 2008, **89**, 890–896.
10 X. Guo, Z. Dai, X. Gong, X. Chen, H. Liu, F. Wang and Z. Yu, Performance of an entrained-flow gasification technology of pulverized coal in pilot-scale plant, *Fuel Process. Technol.*, 2007, **88**, 451–459.
11 F. Scala, Fluidized bed gasification of lignite char with CO_2 and H_2O: a kinetic study, *Proc. Combust. Inst.*, 2015, **35**, 2839–2846.
12 K. Jayaraman and I. Gökalp, Thermal characterization, gasification and kinetic studies of different sized Indian coal and char particles, *International Journal of Advances in Engineering Sciences & Applied Mathematics*, 2014, **6**, 31–40.
13 D. Roberts and D. Harris, A kinetic analysis of coal char gasification reactions at high pressures, *Energy Fuels*, 2006, **20**, 2314–2320.
14 J. Huang, Y. Fang, H. Chen and Y. Wang, Coal gasification characteristic in a pressurized fluidized bed, *Energy Fuels*, 2003, **17**, 1474–1479.
15 P. Li, Q. Yu, Q. Qin and W. Lei, Kinetics of CO_2/Coal Gasification in Molten Blast Furnace Slag, *Ind. Eng. Chem. Res.*, 2012, **51**, 15872–15883.
16 D. Roberts and D. Harris, High-Pressure Char Gasification Kinetics: CO Inhibition of the C–CO_2 Reaction, *Energy Fuels*, 2011, **26**, 176–184.
17 J. Ochoa, M. Cassanello, P. Bonelli and A. Cukierman, CO_2 gasification of Argentinean coal chars: a kinetic characterization, *Fuel Process. Technol.*, 2001, **74**, 161–176.
18 S. Kajitani, S. Hara and H. Matsuda, Gasification rate analysis of coal char with a pressurized drop tube furnace, *Fuel*, 2002, **81**, 539–546.
19 R. C. Everson, H. W. Neomagus, R. Kaitano, R. Falcon and V. M. du Cann, Properties of high ash coal–char particles derived from inertinite-rich coal: II gasification kinetics with carbon dioxide, *Fuel*, 2008, **87**, 3403–3408.
20 M. Malekshahian and J. M. Hill, Kinetic analysis of CO_2 gasification of petroleum coke at high pressures, *Energy Fuels*, 2011, **25**, 4043–4048.
21 S. Kasaoka, Y. Sakata and C. Tong, Kinetic Evaluation of the Reactivity of Various Coal Chars for Gasification with Carbon Dioxide in Comparison with Steam, *Int. Chem. Eng.*, 1984, **25**, 1.
22 C. Shuai, Y.-Y. Bin, S. Hu, J. Xiang, L.-S. Sun, S. Su, K. Xu and C.-F. Xu, Kinetic models of coal char steam gasification and sensitivity analysis of the parameters, *J. Fuel Chem. Technol.*, 2013, **41**, 558–564.
23 J.-L. Zhang, G.-W. Wang, J.-G. Shao and H.-B. Zuo, A Modified Random Pore Model for the Kinetics of Char Gasification, *BioResources*, 2014, **9**, 3497–3507.
24 S. Bhatia and D. Perlmutter, A random pore model for fluid-solid reactions: I isothermal, kinetic control, *AIChE J.*, 1980, **26**, 379–386.
25 I. Ahmed and A. Gupta, Kinetics of woodchips char gasification with steam and carbon dioxide, *Appl. Energy*, 2011, **88**, 1613–1619.
26 I. Sircar, A. Sane, W. Wang and J. P. Gore, Experimental and modeling study of pinewood char gasification with CO_2, *Fuel*, 2014, **119**, 38–46.
27 D. Roberts and D. Harris, Char gasification with O_2, CO_2, and H_2O: effects of pressure on intrinsic reaction kinetics, *Energy Fuels*, 2000, **14**, 483–489.
28 D. Roberts, D. Harris and T. Wall, On the effects of high pressure and heating rate during coal pyrolysis on char gasification reactivity, *Energy Fuels*, 2003, **17**, 887–895.
29 L. Liu, Y. Cao and Q. Liu, Kinetics studies and structure characteristics of coal char under pressurized CO_2 gasification conditions, *Fuel*, 2015, **146**, 103–110.
30 L. Liu, Q. Liu, Y. Cao and W. P. Pan, The isothermal studies of char–CO_2 gasification using the high-pressure thermo-gravimetric method, *J. Therm. Anal. Calorim.*, 2015, **120**, 1877–1882.
31 J. Strange and P. Walker Jr, Carbon–carbon dioxide reaction: Langmuir–Hinshelwood kinetics at intermediate pressures, *Carbon*, 1976, **14**, 345–350.
32 S. Kajitani, Y. Zhang, S. Umemoto, M. Ashizawa and S. Hara, Co-gasification Reactivity of Coal and Woody Biomass in High-Temperature Gasification, *Energy Fuels*, 2009, **24**, 145–151.
33 G. R. Gavals, A random capillary model with application to char gasification at chemically controlled rates, *AIChE J.*, 1980, **26**, 577–585.
34 K. J. Hüttinger and J. S. Nill, A method for the determination of active sites and true activation energies in carbon gasification: (II) experimental results, *Carbon*, 1990, **28**, 457–465.
35 D. G. Roberts, D. J. Harris and T. F. Wall, in High-pressure intrinsic char gasification kinetics: an application of a modified *n*th order rate equation, *International Pittsburgh Coal Conference*, 2001.
36 G.-S. Liu, A. Tate, G. Bryant and T. Wall, Mathematical modeling of coal char reactivity with CO_2 at high pressures and temperatures, *Fuel*, 2000, **79**, 1145–1154.
37 G. Lu and D. Do, A kinetic study of coal reject-derived char activation with CO_2, H_2O, and air, *Carbon*, 1992, **30**, 21–29.
38 D. G. Roberts, E. M. Hodge, D. J. Harris and J. F. Stubington, Kinetics of char gasification with CO_2 under regime II conditions: effects of temperature, reactant, and total pressure, *Energy Fuels*, 2010, **24**, 5300–5308.

39 H. Lorenz, E. Carrea, M. Tamura and J. Haas, The role of char surface structure development in pulverized fuel combustion, *Fuel*, 2000, **79**, 1161–1172.
40 E. Cetin, B. Moghtaderi, R. Gupta and T. F. Wall, Influence of pyrolysis conditions on the structure and gasification reactivity of biomass chars, *Fuel*, 2004, **83**, 2139–2150.
41 M. Zanetti, T. Kashiwagi, L. Falqui and G. Camino, Cone calorimeter combustion and gasification studies of polymer layered silicate nanocomposites, *Chem. Mater.*, 2002, **14**, 881–887.
42 N. M. Laurendeau, Heterogeneous kinetics of coal char gasification and combustion, *Prog. Energy Combust. Sci.*, 1978, **4**, 221–270.
43 D. G. Roberts, D. J. Harris and T. F. Wall, in High-pressure intrinsic char gasification kinetics: an application of a modified *n*th order rate equation, *International Pittsburgh Coal Conference*, 2001.